JCTC Journal of Chemical Theory and Computation

Article

pubs.acs.org/JCTC

How Small Can a Catenane Be?

Xuejun Feng,*[,†] Jiande Gu,*[,‡] Qun Chen,[†] Jenn-Huei Lii,[§] Norman L. Allinger,[⊥] Yaoming Xie,[⊥] and Henry F. Schaefer, III*[,⊥]

[†]School of Petrochemical Engineering, Changzhou University, Changzhou 213164, China

[‡]Drug Design & Discovery Center, State Key Laboratory of Drug Research, Shanghai Institute of Materia Medica Chinese Academy of Science, Shanghai 201203, China

[§]Department of Chemistry, National Changhua University of Education, No. 1, Jin-De Road, Changhua City 50058, Taiwan

[⊥]Center for Computational Chemistry, University of Georgia, Athens, Georgia 30602-2525, United States

Supporting Information

ABSTRACT: Catenanes are playing an increasingly important role in supramolecular chemistry. In attempting to identify the minimum number of carbon atoms in a viable catenane, the B3LYP, BP86, M06-2X, MM3, and MM4 methods were applied to study representative [2]catenane models, which consist of two mechanically interlocked saturated *n*-cycloalkanes ($[C_nH_{2n}]_2$). The structures, energy variations, and electron density differences vary nearly monotonically from n = 18 to 11. For example, the B3LYP/DZP++ dissociation energies $[C_nH_{2n}]_2 \rightarrow 2C_nH_{2n}$ are 101, 121, 159, 191, 222, 252, 290, and 323 kcal/mol from n = 18 to 11, respectively. However, there is much variation among the energetic predictions with the B3LYP, BP86, M06-2X, MM3, and MM4 methods. The distances of the longest C−C single bond in each catenane are 1.593 (n = 18), 1.604 (n = 17), 1.631 (n = 16), 1.640 (n = 15), 1.667 (n = 14), 1.669 (n = 13), 1.680 (n = 12), and 1.689 Å (n = 11). These results display something of a shoulder in the vicinity of n = 14. This may suggest that $[C_{15}H_{30}]_2$ is the smallest catenane that will resist fragmentation under specified laboratory conditions.

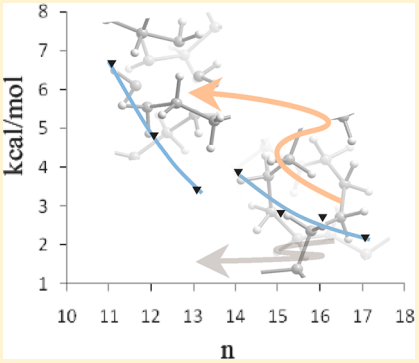

INTRODUCTION

Molecules of knot structure have attracted the interest of chemists for decades.[1] The saturated hydrocarbon catenanes are one example of numerous such families of molecules. A catenane is a compound consisting of two interlocking rings. These mechanically interlocked molecules continue to be attractive research targets due to their unique topologies and their potential to function as molecular machines.[1,2]

The research field of knot structure molecules and its related molecules goes back more than five decades.[2] The report by Wasserman[3] in 1960 of the synthesis of a [2]catenane heralded the beginning of practical approaches for the creation of a large collection of mechanically interlocked molecules.[4−23] Molecular knot research has remained very active, mostly in relation to the novel properties (such as electron transfer, controlled motions, mechanical properties, mechanical bonds, etc.) that these compounds may exhibit.[14−18] In addition, molecular knots represent attractive synthetic challenges in chemistry.[16,19] In response to the desire to take on substantially more demanding synthetic challenges, chemists have been working on the task of designing (often with the aid of computational research) and synthesizing more and more complicated molecular knots.[19] Recently, Leigh and colleagues[20] reported the synthesis of the first non-DNA molecular knot of higher order, namely the pentafoil knot, through a one-step strategy. Their rational strategy for making a molecular pentafoil knot combined several aspects of modern supramolecular chemistry, including metal-directed assembly, anion templation, and reversible covalent bond formation.

Computer simulations have been carried out to elucidate the formation of molecular knots at the atomic level. A trefoil knotting structure was predicted as early as 1992 by Schlick and Olson by large time-step dynamics simulation of supercoiled DNA.[24] This simulation also detailed a supercoiled-directed knotting mechanism. To explore the possible minimum number of carbon atoms for a trefoil in a polymer strand, Car−Parrinello molecular dynamics (CPMD) simulations were performed by Klein and colleagues in 1999.[25] By systematically increasing the separation between the terminal carbon atoms, Klein studied the response of the *n*-decane molecule to uniaxial strain and concluded that 23 carbon atoms comprise the tightest knot that can be sustained in a polyethylene strand without breaking.

The understanding of the structure and properties of knots at the atomic level is still less than adequate. Even though catenanes are now commonplace and available in gram scale quantities,[21−23] the smallest number of carbon atoms that can be sustained as a catenane is still not well-established. In attempting to identify this minimum structural assembly in catenanes, second-order perturbation theory, density functional, and molecular mechanics methods were applied in our

Received: October 23, 2013
Published: February 25, 2014

   dx.doi.org/10.1021/ct400926p | J. Chem. Theory Comput. 2014, 10, 1511−1517

laboratories. As a representative [2]catenane system, molecules with two mechanically interlocked saturated *n*-cycloalkanes ($[C_nH_{2n}]_2$) were adopted in the present study. Due to its great simplicity, this system is an excellent generic model for the examination of the fundamental properties of a molecular knot.

METHODS

Over the last two decades, density functional theory (DFT) has become a reliable modeling method for predicting geometries and energetic properties of relatively large molecular systems. Among various functionals, the correlation functional of Lee, Yang, and Parr (LYP)[26,27] in conjunction with Becke's three-parameter HF/DFT functional (B3),[28] B3LYP, has been the most widely used in the investigation of the physical properties of organic molecules. Other functionals such as BP86[29,30] and newly developed Minnesota density functional, M06-2X,[31] have also been widely applied in the computational study of relatively large molecules. To evaluate the reliability of the predictions, all three functionals, B3LYP, BP86, and M06-2X, were applied in the present research. Basis sets of double-ζ quality associated with polarization and diffuse functions,[32] namely DZP++, were adopted in the DFT calculations. Previous studies have revealed that the basis set dependence of DFT functionals is fairly small and a DZP++ quality basis set is sufficient for most molecular systems.[32] Harmonic vibrational frequencies for all of the complexes were determined analytically. The Møller–Plesset correlation energy truncated at second-order (MP2) method with the DZP basis set was applied in the geometric optimization study and the energetic property investigations. The DFT and MP2 computations were performed using the Gaussian-09 package of programs.[33] All the structures reported in this paper refer to the lowest-lying D_2 conformers, which have been confirmed by the random-kick conformer search with molecular mechanics (MM3/MM4) methods.[34]

RESULTS AND DISCUSSION

Structures of the models were fully optimized with the DFT/DZP++ method. Analysis of the results showed that the three functionals used in this investigation yield similar geometric parameters (see Figure 1 and Table 1–3 in the Supporting Information, SI) and similar energetic properties (Table 4 in the SI). Therefore, the discussion below is primarily based on the results obtained by the B3LYP/DZP++ approach.

Geometries. All the structures in this study are subjected to be the local minima on the potential energy surface. Those with imaginary frequencies will not be considered below. For clarity, structures are limited to those with D_2 symmetry in this research. With this constraint, the optimized structures of the [2]catenanes of $[C_nH_{2n}]_2$ (n = 11–18) can be cataloged in two classes according to the geometric arrangement of the interlock patterns (Figure 1). The first class is that for which the closest units between the interlocked rings are $-CH_2-$ units (A in Figure 1), and the second pattern occurs when the most closest units are the C–C bonds (B in Figure 1). Vibrational frequency analyses reveal that the all the optimized structures (D_2 symmetry) with the first interlock pattern A are genuine minima for n = 11–18. On the other hand, structures with the second interlock pattern B are not local minima on the potential energy surface when n is larger than 14. Moreover, the energies of conformers with the first interlock pattern are lower than the corresponding second interlock conformers. Therefore, the discussion below will be focused on the structures belonging to the first class only. Figure 2 depicts these optimized structures, and their C–C distances are reported in Table 1.

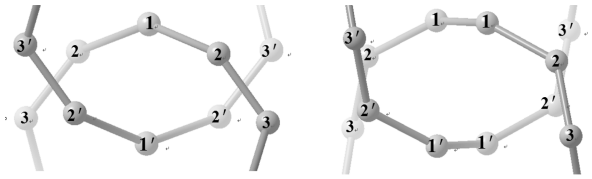

Figure 1. Geometric arrangement of interlocking patterns for the two types of catenanes. (A) The closest units between the interlocked rings are the $-CH_2-$ segments. (B) The closest units between the interlocked rings are the C–C bonds. H atoms are not shown for clarity. The labels shown here are adopted in the text.

The C–C bonds in the interlocked complexes are found to be significantly longer than those in the separated rings. This phenomenon is more profound when the size of the ring is small, as seen in Table 1. For our model **11–11**, the C–C bond lengths range from 1.599 to 1.691 Å, while they are 1.542–1.558 Å (see Table 1 in the SI) in the corresponding single ring molecule. This bond distance extension may be attributed to the high degree of stress caused by the compact packing in the catenanes. However, this elongation in bond length decreases as the number (n) of the carbon atoms increases. For n = 18, the C–C length varies from 1.549 to 1.593 Å.

Without exception, the longest C–C bond length is C1—C2 (Figure 2 and Table 1), suggesting that the C–C bond is weak when one of carbon atom resides near the center of the other ring molecule. Examining the structures of the interlocked molecules reveals that the C1—C2 distances range from 1.593 Å (**18–18**) to 1.691 Å (**11–11**). These extended C–C bonds are significantly longer than those for the isolated cycloalkanes (1.533–1.558 Å). The C1—C2 distances increase fairly evenly from 1.593 to 1.681 Å as the number of carbon atoms in a ring decreases from 18 to 14. This monotonic trend breaks when n goes from 14 to 13, and the C1—C2 distance in **13–13** is 1.670, 0.011 Å less than that of **14–14**. As n is reduced from 13 to 11, the C1—C2 bond elongation resumes at a relative small rate (from 1.670 to 1.691 Å, Figure 3). The changes in C1—C2 bond distance suggest that n = 14 is a critical point for sustaining a conventional C1—C2 bond in the catenanes. This trend is consistent with the further observation of the variations of the successive C–C bond distance (C2—C3). A large rate of increase is found in the C2—C3 bond length as n deceases from 18 (1.550 Å) to 14 (1.605 Å), while a much smaller change is seen from 13 (1.604 Å) to 11 (1.611 Å). Also, the same C2—C3 bond length is predicted for **13–13** and **14–14** (see Figure 3). These C–C distance changes support the proposition that n = 14 is a special point for the catenanes modeled here.

The separation between the two interlocked rings may be represented by the atomic distance C1—C1′. Here C1 is the carbon atom at the crossing point of one cycloalkane ring and C1′ is that of the other ring (see Figure 1). Figure 4 depicts the C1—C1′ distances of the models of catenanes with n = 11–18. The C1—C1′ distance varies from 2.334 to 2.607 Å as n increases from 11 to 14, and this distance further increases from 2.607 to 3.938 Å between 14 and 18. Consistent with the trends of C–C bonds discussed above, changes in the C1—C1′

dx.doi.org/10.1021/ct400926p | J. Chem. Theory Comput. 2014, 10, 1511–1517

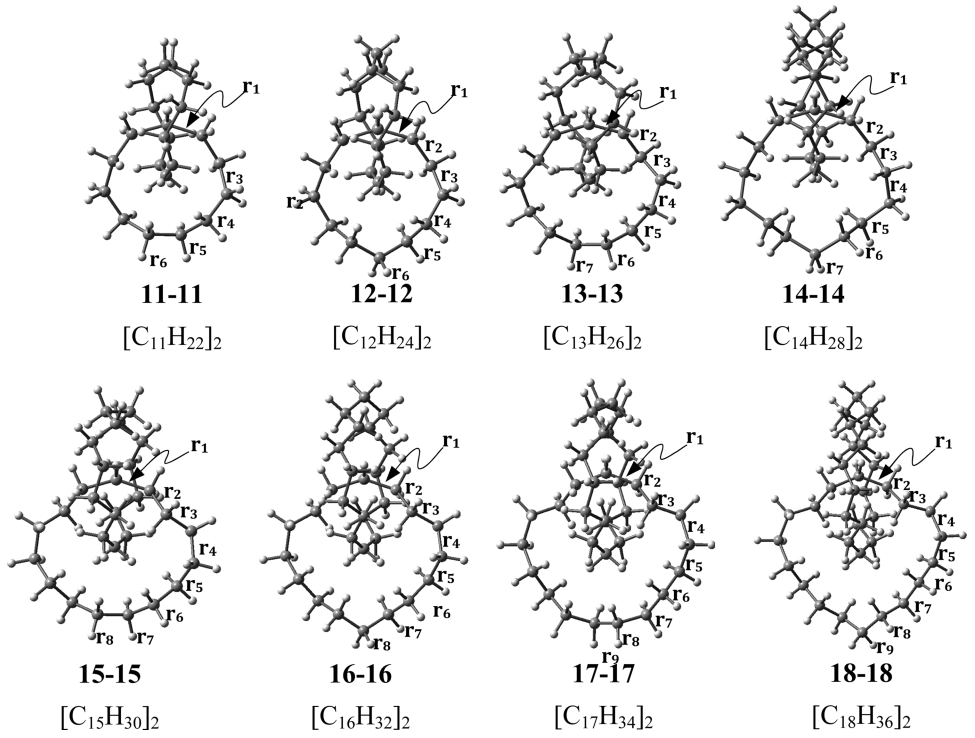

Figure 2. Optimized structures for the catenanes $[C_nH_{2n}]_2$ (n = 11−18).

Table 1. C−C Atomic Distances of the Optimized Structures of $[C_nH_{2n}]_2$ (n = 11−18)[a]

	11−11 $[C_{11}H_{22}]_2$	12−12 $[C_{12}H_{24}]_2$	13−13 $[C_{13}H_{26}]_2$	14−14 $[C_{14}H_{28}]_2$	15−15 $[C_{15}H_{30}]_2$	16−16 $[C_{16}H_{32}]_2$	17−17 $[C_{17}H_{34}]_2$	18−18 $[C_{18}H_{36}]_2$
r_1	1.691	1.681	1.670	1.681	1.641	1.632	1.605	1.593
r_2	1.611	1.609	1.604	1.605	1.578	1.569	1.553	1.550
r_3	1.608	1.596	1.576	1.569	1.564	1.562	1.552	1.550
r_4	1.612	1.590	1.574	1.560	1.570	1.571	1.563	1.561
r_5	1.594	1.572	1.571	1.560	1.573	1.571	1.566	1.565
r_6	1.599	1.573	1.576	1.551	1.565	1.562	1.555	1.551
r_7			1.569	1.558	1.569	1.556	1.565	1.556
r_8					1.568	1.554	1.564	1.549
r_9							1.562	1.554

[a]Structures were optimized at the B3LYP/DZP++ level of theory. The structural parameters by the BP86, M06-2X, and MP2 approaches are similar. Atomic distances are in angstroms.

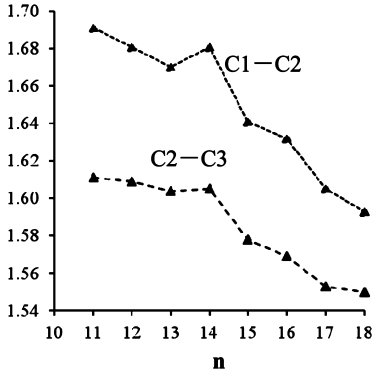

Figure 3. C1—C2 (r_1 in Table 1) and C2—C3 (r_2 in Table 1) bond distances for the optimized structures of the catenanes $[C_nH_{2n}]_2$ (n = 11−18). Bond lengths are in angstroms.

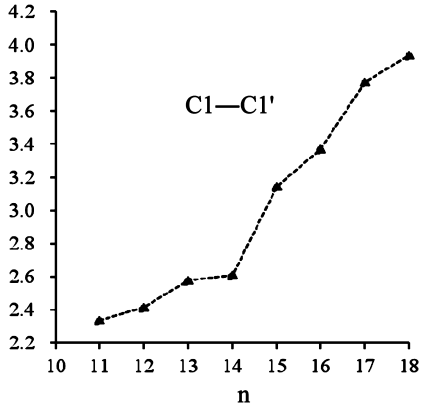

Figure 4. C1—C1′ atomic distance of the optimized structures of $[C_nH_{2n}]_2$ (n = 11−18), where C1 is the atom point of closest approach of the carbon of one ring and C1′ is that of the other ring. The distances are in angstroms.

atomic distance show a bit of a shoulder at n = 14. The trend in Figure 4 also confirms that the carbon atoms of different rings move away from each other once there is sufficient space.

dx.doi.org/10.1021/ct400926p | J. Chem. Theory Comput. 2014, 10, 1511−1517

To further confirm that n = 14 is somewhat unusual for the $[C_nH_{2n}]_2$ models of [2]catenanes, the distance between the geometric centers of each ring was examined. This geometric center here was the average of the positions of the nuclei of the carbon atoms in each ring. As n increases from 11 to 14, the center−center distance monotonically increases from 3.045 to 3.828 Å as shown in Figure 5. It is quite interesting that for n = 14−18 this center−center distance oscillates (between 3.6 and 3.9 Å, approximately). This zigzag pattern seems to suggest that the space between the two rings is sufficient for the coexistence of the two interlocked rings. The variation pattern of the ring-center distances versus the numbers of carbon atoms again suggests that n = 14 is an inflection point for the transformation of the catenanes examined.

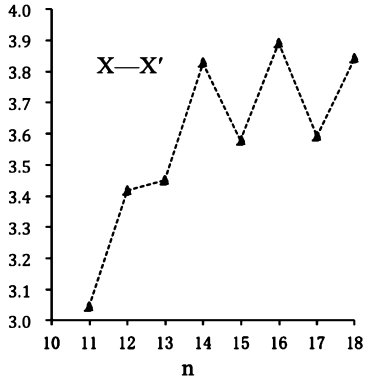

Figure 5. Ring-center (X—X′) distance of the optimized structures of $[C_nH_{2n}]_2$ (n = 11−18), where X is the geometric center of one ring and X′ is that of the other ring. Distances are in angstroms.

As mentioned above, compared to the standard C−C bond (1.533−1.558 Å) in the conventional cycloalkanes, the C1—C2 bonds in the cantenes (n = 11−14) are much longer. The long C1—C2 atomic distances (1.670−1.691 Å) in these models suggest that the C1 and C2 atoms are less strongly bound than a conventional C−C bond. At high temperatures, thermal motion might be expected to rupture these weakened bonds. This elongation is also extended to the neighboring C2—C3 bonds, as shown in Figure 3. However, the increases for the C2—C3 bond distances are less than those for the C1—C2 bonds. Thus, bond breaking may be expected for the C1—C2 bonds of the catenanes with $n \leq 14$. Experiments have revealed that the breakage in a knotted rope usually takes place at the point just outside the "entrance" to the knot.[35] CPMD simulation studies by Klein et al.[25] suggested that the two strands cross each other with the least separation at this position. The qualitative picture presented by Klein resembles that drawn for the catenanes in the present study.

Energetic Properties. The interlocking of small rings necessarily causes greater stress in these systems. Thus, the fragment energy of each CH_2 unit (E_n/n) increases as the number of carbon atoms of the cycloalkane decreases. To examine the relationship between the energy and the size of the system, the energy variation has been defined as $\Delta E(n, n+1) = E_n/n - E_{n+1}/(n+1)$, where E_n is the energy of the modeled catenane with two interlocked n-membered rings (n = 11−17). Figure 6 illustrates the trends in the energy change with respect to the number of carbon atoms in each ring. In general, $\Delta E(n, n+1)$ vs. n can be divided into two sections. When n is reduced from 17 to 14, the energy change per CH_2 unit increases from 2.0 to 2.9 kcal/mol. When n is reduced from 14 to 11, $\Delta E(n, n+1)$ increases from 2.9 to 6.5 kcal/mol, as predicted at the B3LYP/DZP++ level of theory. Other approaches, such as M06-2X and MP2, also envisage the general trend seen in Figure 6.

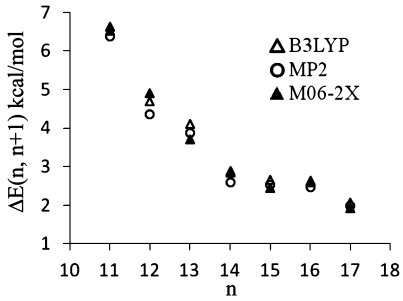

Figure 6. Trends of the energy change $\Delta E(n, n+1) = E_n/n - E_{n+1}/(n+1)$, ($n$ = 11−17), with respect to the number of the carbon atoms in the ring (n).

Compared to the isolated rings, the interlocked complexes are invariably higher in energy. Table 2 and Figure 7 show the variations of the interaction energy E_{inter} as a function of n, in which the interaction energy E_{inter} is defined by the reaction $2C_nH_{2n} \rightarrow [C_nH_{2n}]_2$. The trend of monotonic change of interlocking energies shows a slight break between n = 13 and 14, as illustrated in Figure 7. The pattern of the energy change and that of the interlocking energy hint at a transition between n = 13 and 14 (although not convincingly in Figure 7). It is clear that the interaction energies E_{inter} predicted by the B3LYP and BP86 approaches are systematically higher than those from

Table 2. Interaction Energies E_{inter} (= $E[C_nH_{2n}]_2 - 2E[C_nH_{2n}]$) (kcal/mol) Predicted by Different Computational Methods

	B3LYP	BP86	M06-2X	MP2	MM3	MM4
11−11	325.2	302.3	298.9	286.8	292.4	262.5
12−12	292.2	271.6	261.9	253.2	283.2	252.2
13−13	254.1	236.5	211.9	216.9	253.7	228.7
14−14	224.7	208.5	193.7	188.1	220.1	205.0
15−15	193.8	180.7	160.6	158.6	197.3	181.7
16−16	161.5	150.0	126.6	122.8	174.7	160.9
17−17	132.8	123.1	96.1	94.3	136.1	127.4
18−18	103.7	96.4	67.2	64.4	108.2	99.4

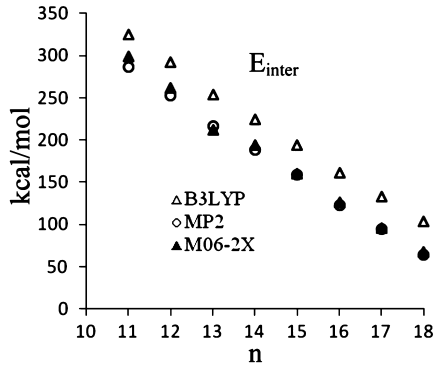

Figure 7. Variation of the interaction energy, E_{inter}, with respect to the number of carbon atoms in the ring (n) predicted by the B3LYP, M06-2X, and MP2 methods. E_{inter} is the difference between the energies of $[C_nH_{2n}]_2$ and two separated C_nH_{2n} molecules.

dx.doi.org/10.1021/ct400926p | J. Chem. Theory Comput. 2014, 10, 1511−1517

the M06-2X and MP2 methods. Recalling that the atomic distances between the interlocked atoms (C1 and C1′) range from 2.3 to 4.0 Å, one might expect dispersion interactions in the interlocking area. The systematic large interaction energies at the B3LYP (and BP86) level of theory could be the result of inadequacy of these functionals for the dispersion interaction zone. On the other hand, the M06-2X and MP2 methods predict an attractive dispersion interaction in the interlocking area and therefore result in relatively small E_{inter} (as compared to the B3LYP and BP86 results).

The variations in the interaction free energies G_{inter} follow similar trends, as shown in Figure 8 and Table 3. At absolute

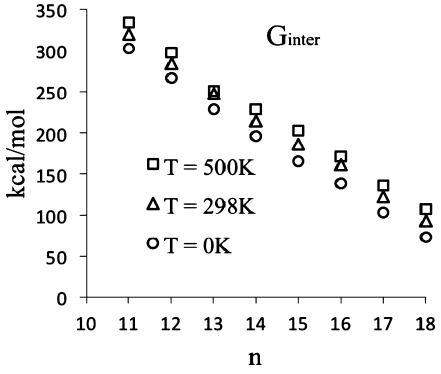

Figure 8. Variation of the interaction free energy, G_{inter}, with respect to the number of carbon atoms in the ring (n) predicted by the M06-2X method at different temperatures.

Table 3. Interaction free energies G_{inter} (= $G[C_nH_{2n}]_2 - 2G[C_nH_{2n}]$) (kcal/mol) at T = 0, 298, and 500 K, Predicted by the B3LYP and M06-2X Approaches

	B3LYP			M06-2X		
	0 K	298 K	500 K	0 K	298 K	500 K
11−11	329.5	347.1	358.3	302.9	320.2	333.7
12−12	295.0	313.4	328.3	266.5	284.0	297.7
13−13	258.1	276.0	288.8	228.9	247.7	251.1
14−14	225.0	242.2	256.5	196.4	214.5	228.8
15−15	195.4	213.0	228.6	165.9	186.3	202.9
16−16	168.5	186.5	197.7	139.2	161.3	171.5
17−17	136.1	154.9	170.6	103.3	122.3	136.1
18−18	105.2	124.2	164.9	73.3	93.2	107.4

zero temperature, G_{inter} (that is, the ZPE-corrected E_{inter}) displays a minor but recognizable irregularity between n = 13 and 14. This trend increases as the temperature rises, as may be seen from Figure 8 (T = 500 K).

It is important to examine the variations in the interaction entropy (S_{inter}) vs. the size of the ring in order to predict the favorability of the catenanes (Figure 9). The increases in the entropy corresponding to the formation of two separated rings from the interlocked ring assembles ($-S_{inter}$) are predicted to range from 59 to 82 cal/(mol K) (M06-2X method). Although the quantitative accuracy of the computed entropies is limited by the methods applied to the present systems, the trends of the entropy increases can be estimated qualitatively. In general, this entropy increase is around 63 to 65 cal/(mol K) for n = 11−14, while it is around 65 to 82 cal/(mol K) for n = 14−18. Thus, increasing the temperature is expected to have significant influence on the stability of the catenanes with n larger than 14.

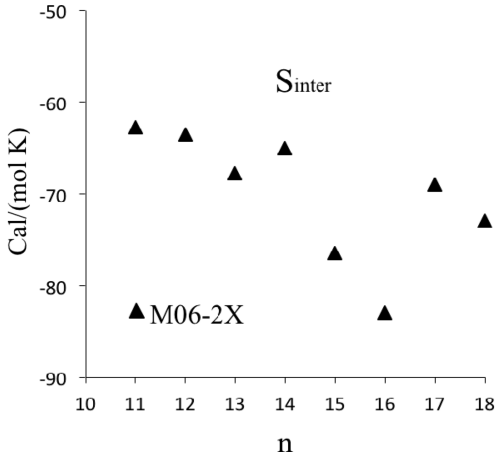

Figure 9. Variation of the interaction entropy, S_{inter}, with respect to the number of carbon atoms in the ring (n) predicted by the M06-2X method.

Since the entropy increases for destabilization of the interlocked rings are small, especially for the interlocked complexes with n less than 14, the contribution of the entropy to the free energy G_{inter} is very small. At T = 298 K, the free energy increase due to the entropy is about 20 kcal/mol. Therefore, the high tension of geometric stress caused by the compact packing dominates the high free energy of the interlocked catenanes.

Electron Density Considerations. To examine the variations caused by the interlocking interactions between the rings, electron density differences between the catenane molecules and the corresponding separated ring molecules are mapped in Figure 10. From the electron density difference map (or electron density deformation map) on the plane C2—C1—C2 for **11−11**, one may see that the electron density decreases around atom C1 while it increases around the other carbon atoms in the catenane. This change may also be seen from the natural population analysis of the charge of the systems (see Table 5 of the SI). A similar density deformation pattern is observed for **12−12**, **13−13**, and **14−14**. However, the electron density deformations in the complexes with n > 14 are of lesser magnitude.

It is very interesting to note that, due to the interlocking moieties, along the C1—C2 bond the electron density decreases dramatically on the C1 side while it increases significantly on the C2 side, as shown in the electron density deformation map for **11−11**. This deformation suggests that the electron density shifts to the C2 atoms (from the C1 atom) in the interlocked system. Thus, the covalent bond structure of C1—C2 is disturbed greatly in this situation. On the other hand, the charge shifts also imply that the CH_2 unit is bound between the two C2 atoms through charge−charge interactions in the interlocked model.

CONCLUDING REMARKS

All the properties explored in the present study—geometrical parameters, energetics, natural bond orbital (NBO) analyses, and electron density deformations—point to n = 14 as a shoulder for the catenane models $[C_nH_{2n}]_2$. The analysis of the electron density deformation maps reveals that the normal C1—C2 covalent bond structure is gradually altered for the complexes as a function of n. The interlocked cycloalkanes are expected to rupture at the crossing point, perhaps when the

dx.doi.org/10.1021/ct400926p | J. Chem. Theory Comput. 2014, 10, 1511−1517

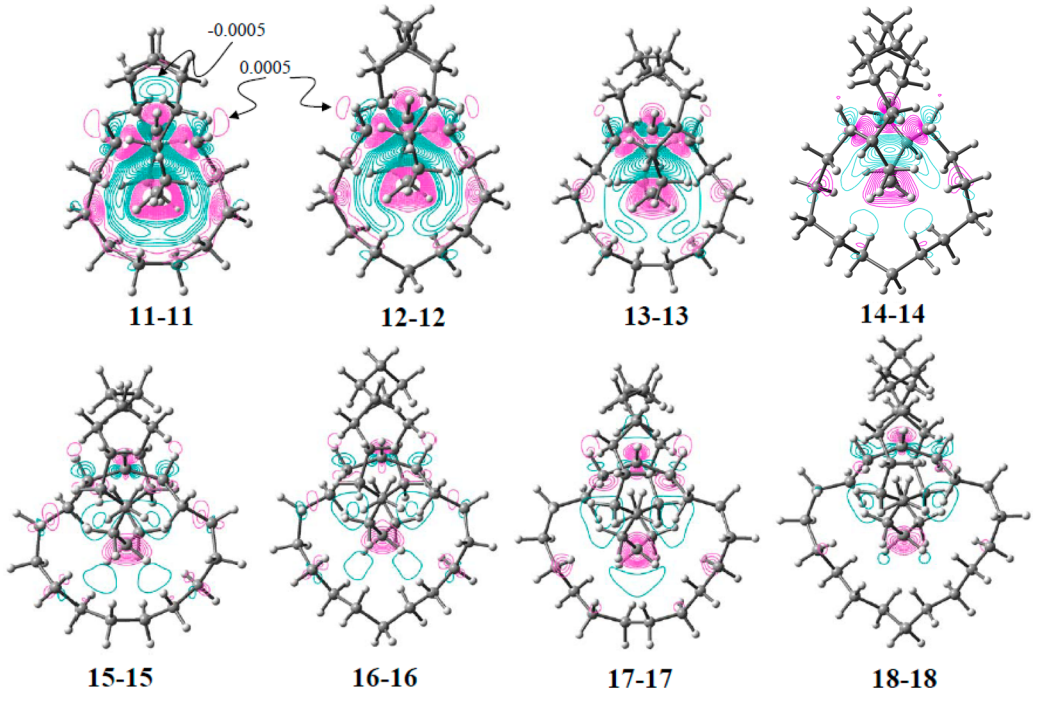

Figure 10. Electron density deformation maps ($\Delta\rho$) of the modeled catenanes $[C_nH_{2n}]_2$ (n = 11−18), where $\Delta\rho = \rho([C_nH_{2n}]_2) - 2\rho(C_nH_{2n})$. Increments between two contiguous contour lines are 0.0005 au. Color representations: pink for increase, light blue for decrease in electron density.

number of CH_2 units in the alkane rings is reduced to 14. It is the compact packing that is the driving force for the bond weakening.

It should be noted that, in the present models, two C−C bond contractions as a function of n occur in parallel. Since the energy for breaking two C−C bonds is approximately twice that needed to break one bond, one should expect that much less strain could cause ring rupture in the interlocked systems compared to the separated cycloalkanes.

Finally, there is considerable energy stored in the $[C_nH_{2n}]_2$ type catenanes, and of course, this decreases with n. The geometric stress tension caused by the compact packing dominates the high free energy of the interlocked catenanes. The synthesis of these compounds would be a great challenge for experimental investigations.

■ ASSOCIATED CONTENT

Supporting Information

The optimized structures, energies, and charge distributions for $[C_nH_{2n}]_2$ (n = 11−18). This material is available free of charge via the Internet at http://pubs.acs.org.

■ AUTHOR INFORMATION

Corresponding Authors

*X.F.: xuejun_f@hotmail.com.
*J.G.: jiande@icnanotox.org.
*H.F.S.: qc@uga.edu.

Notes

The authors declare no competing financial interest.

■ ACKNOWLEDGMENTS

This work in China was supported by the Priority Academic Program Development of Jiangsu Higher Education Institutions, China and the U.S. National Science Foundation (Grant CHE-1054286).

■ REFERENCES

(1) Schill, G. *Catenanes, Rotaxanes and Knots*; Academic Press: New York and London, 1971.
(2) (a) Durola, F.; Sauvage, J. -P.; Wenger, O. S. *Coord. Chem. Rev.* **2010**, *254*, 1748−1759. (b) Sauvage, J. -P.; Gaspard, P. *From Non-Covalent Assemblies to Molecular Machines*; Wiley-VCH: Weinheim, 2010.
(3) Wasserman, E. *J. Am. Chem. Soc.* **1960**, *82*, 4433−4434.
(4) Amabilino, D. B.; Stoddart, J. F. *Chem. Rev.* **1995**, *95*, 2725−2828.
(5) Sauvage, J.-P.; Dietrich-Buchecker, C. *Molecular Catenanes, Rotaxanes and Knots*; Wiley-VCH: Weinheim, 1999.
(6) Raymo, F. M.; Stoddart, J. F. *Chem. Rev.* **1999**, *99*, 1643−1663.
(7) Fujita, M. *Acc. Chem. Res.* **1999**, *32*, 53−61.
(8) Collin, J. P.; Dietrich-Buchecker, C.; Gavina, P.; Jiminez-Molero, M. C.; Sauvage, J.-P. *Acc. Chem. Res.* **2001**, *34*, 477−487.
(9) Dietrich-Buchecker, C. O.; Sauvage, J.-P.; Kern, J.-M. *J. Am. Chem. Soc.* **1984**, *106*, 3043−3045.
(10) Kaiser, G.; Jarrosson, T.; Otto, S.; Ng, Y.-F.; Bond, A. D.; Sanders, J. K. M. *Angew. Chem., Int. Ed.* **2004**, *43*, 1959−1962.
(11) Wang, L.; Vysotsky, M. O.; Bogdan, A.; Bolte, M.; Bohmer, V. *Science* **2004**, *304*, 1312−1314.
(12) Schalley, C. A.; Weilandt, T.; Bruggermann, J.; Vogtle, F. *Top. Curr. Chem.* **2004**, *248*, 141−200.
(13) Vickers, M. S.; Beer, P. D. *Chem. Soc. Rev.* **2007**, *36*, 211−225.
(14) Stoddart, J. F. *Chem. Soc. Rev.* **2009**, *38*, 1802−1820.
(15) Olson, M. A.; Botros, Y. Y.; Stoddart, J. F. *Pure Appl. Chem.* **2010**, *82*, 1569−1574.
(16) Sauvage, J.-P.; Collin, J. P.; Durot, S.; Frey, J.; Heitz, V.; Sour, A.; Tock, C. *C. R. Chim.* **2010**, *13*, 315−328.
(17) Stoddart, J. F.; Colquhoun, H. M. *Tetrahedron* **2008**, *64*, 8231−8263.
(18) Meyer, C. D.; Forgan, R. S.; Chichak, K. S.; Peters, A. J.; Tangchaivang, N.; Cave, G. W. V.; Khan, S. I.; Cantrill, S. J.; Stoddart, J. F. *Chem.—Eur. J.* **2010**, *16*, 12570−12581.
(19) Lukin, O.; Vogtle, F. *Angew. Chem., Int. Ed.* **2005**, *44*, 1456−1477.
(20) Ayme, J.-F.; Beves, J. E.; Leigh, D. A.; McBurney, R. T.; Rissanen, K.; Schultz, D. *Nature Chem.* **2012**, *4*, 15−20.

(21) Goldup, S. M.; Leigh, D. A.; Long, T.; McGonigal, P. R.; Symes, M. D.; Wu, J. *J. Am. Chem. Soc.* **2009**, *131*, 15924−15929.
(22) Spruell, J. M.; Coskun, A.; Friedman, D. C.; Forgan, R. S.; Sarjeant, A. A.; Trabolsi, A.; Fahrenbach, A. C.; Barin, G.; Paxton, W. F.; Dey, S. K.; et al. *Nature Chem.* **2010**, *2*, 870−879.
(23) Forgan, R. S.; Wang, C.; Friedman, D. C.; Spruell, J. M.; Stern, C. L.; Sarjeant, A. A.; Cao, D.; Stoddart, J. F. *Chem.—Eur. J.* **2012**, *18*, 202−212.
(24) Schlick, T.; Olson, W. K. *Science* **1992**, *257*, 1110−1115.
(25) Saitta, A. M.; Soper, P. D.; Wasserman, E.; Klein, M. L. *Nature* **1999**, *399*, 46−48.
(26) Lee, C.; Yang, W.; Parr, R. G. *Phys. Rev. B* **1988**, *37*, 785−789.
(27) Miehlich, B.; Savin, A.; Stoll, H.; Preuss, H. *Chem. Phys. Lett.* **1989**, *157*, 200−206.
(28) Becke, A. D. *J. Chem. Phys.* **1993**, *98*, 5648−5652.
(29) Perdew, J. P. *Phys. Rev. B* **1986**, *33*, 8822−8824.
(30) Backe, A. D. *Phys. Rev. A* **1988**, *38*, 3098−3100.
(31) Zhao, Y.; Truhlar, D. G. *Theor. Chem. Acc.* **2008**, *120*, 215−241.
(32) Rienstra-Kiracofe, J. C.; Tschumper, G. S.; Schaefer, H. F.; Nandi, S.; Ellison, G. B. *Chem. Rev.* **2002**, *102*, 231−282.
(33) Frisch, M. J.; Trucks, G. W.; Schlegel, H. B.; Scuseria, G. E.; Robb, M. A.; Cheeseman, J. R.; Scalmani, G.; Barone, V.; Mennucci, B.; Petersson, G. A., et al. *Gaussian 09*, Revision A.1; Gaussian, Inc.: Wallingford CT, 2009.
(34) (a) Allinger, N. L.; Yuh, Y. H.; Lii, J.-H. *J. Am. Chem. Soc.* **1989**, *111*, 8551. (b) Allinger, N. L.; Chen, K.; Lii, J.-H. *J. Comput. Chem.* **1996**, *17*, 642.
(35) Ashley, C. W. *The Ashley Book of Knots*; Doubleday: New York, 1993.